ANALYSIS OF HYDRATED CEMENTS USING A SCANNING ELECTRON MICROSCOPE-ENERGY DISPERSIVE X-RAY SPECTROMETER COMBINATION

DECEMBER 1971 - NUMBER 21

BY

SIDNEY DIAMOND

JHRP

JOINT HIGHWAY RESEARCH PROJECT

PURDUE UNIVERSITY AND

INDIANA STATE HIGHWAY COMMISSION

Technical Paper

ANALYSIS OF HYDRATED CEMENTS USING A SCANNING ELECTRON MICROSCOPE - ENERGY DISPERSIVE X-RAY SPECTROMETER COMBINATION

by

Sidney Diamond
Research Associate

Joint Highway Research Project
File: 5-14-5
Project: C-36-61E

Prepared as Part of an Investigation
Conducted by
Joint Highway Research Project
Engineering Experiment Station
Purdue University
In cooperation with the
Indiana State Highway Commission
and the
U.S. Department of Transportation
Federal Highway Administration

Purdue University
Lafayette, Indiana
December 28, 1971

Technical Paper

ANALYSIS OF HYDRATED CEMENTS USING A SCANNING ELECTRON MICROSCOPE - ENERGY DISPERSIVE X-RAY SPECTROMETER COMBINATION

TO: J. F. McLaughlin, Director
Joint Highway Research Project

December 28, 1971

Project: C-36-61E

FROM: H. L. Michael, Associate Director
Joint Highway Research Project

File: 5-14-5

The attached Technical Paper "Analysis of Hydrated Cements Using a Scanning Electron Microscope - Energy Dispersive X-Ray Spectrometer Combination"has been authored by Dr. Sidney Diamond of our staff. The paper is from research performed under the HPR Part II project titled "Fundamental Studies of Portland Cement Concrete".

The paper was presented in May 1971 at a Meeting of the American Ceramic Society and permission of all sponsors to make the presentation was obtained on the basis of an abstract. The paper is now submitted in its entirety for approval of publication in Cement and Concrete Research.

The paper will also be submitted for review, comment and approval of publication to the ISHC and the FHWA.

Respectfully submitted,

Harold L. Michael

Harold L. Michael
Associate Director

HLM:ms

cc:
W. L. Dolch
W. H. Goetz
W. L. Grecco
M. J. Gutzwiller
G. K. Hallock
M. E. Harr
R. H. Harrell
M. L. Hayes
R. D. Miles
J. W. Miller
C. F. Scholer
M. B. Scott
W. T. Spencer
J. A. Spooner
N. W. Steinkamp
H. R. J. Walsh
K. B. Woods
E. J. Yoder

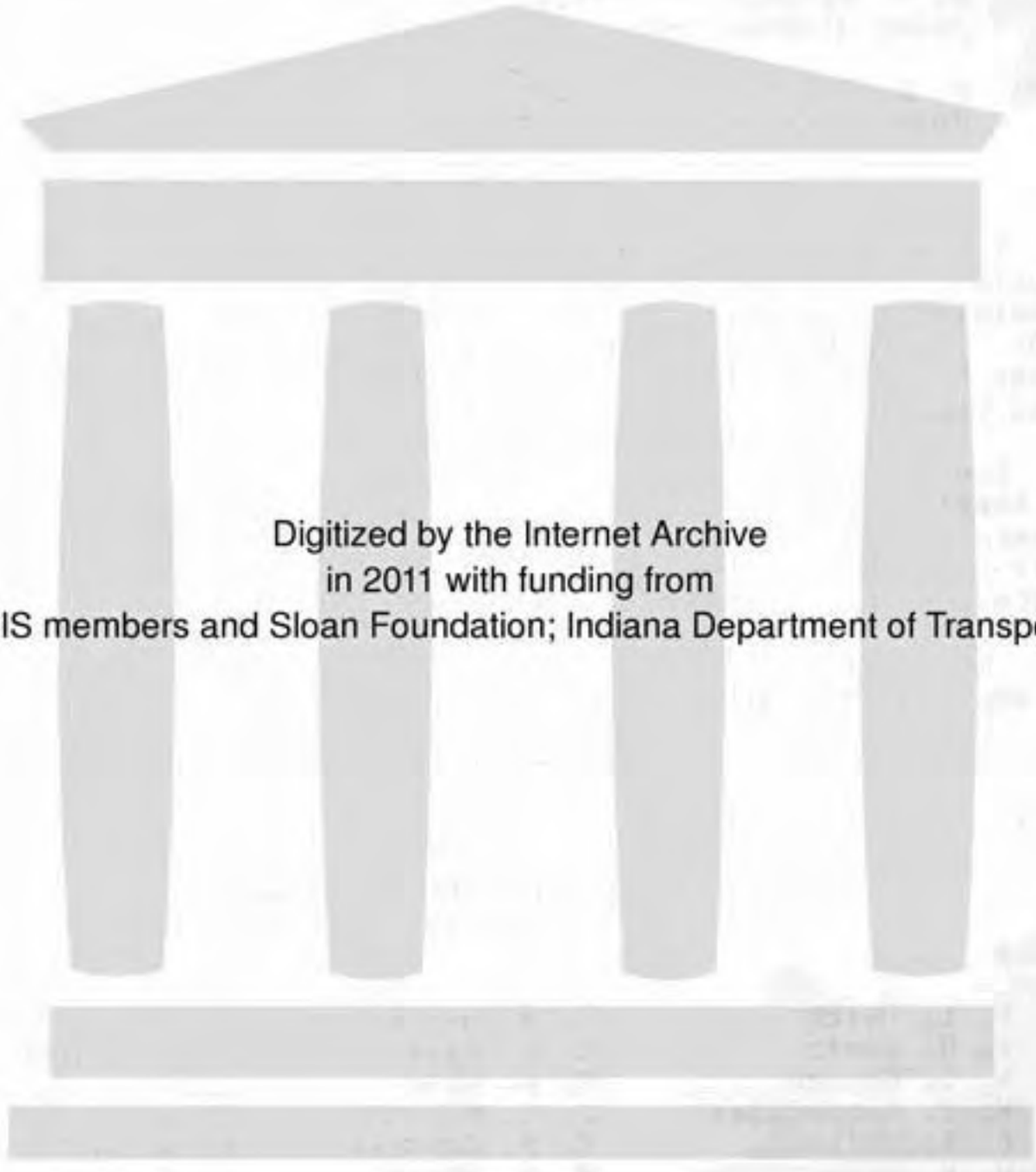

ANALYSIS OF HYDRATED CEMENTS USING A SCANNING ELECTRON MICROSCOPE - ENERGY DISPERSIVE X-RAY SPECTROMETER COMBINATION

by Sidney Diamond
School of Civil Engineering
Purdue University, Lafayette, Indiana 47907, U. S. A.

ABSTRACT

Preliminary studies of the chemical composition of individual particles and other local microstructural units in hydrated Portland cement pastes were carried out using a scanning electron microscope-energy dispersive x-ray spectrometer combination. Calibration curves were prepared in terms of gross peak heights for calcium as compared with silicon, sulfur, and aluminum Kα peaks, for a series of pure homogeneous cement and hydrated cement compounds used as standards. The count ratio was in each case found to be linearly related to the compositional (mole) ratio. The analysis of small (approximately 1½ μm diameter) areas of fracture surface of specimens observed in the SEM was carried out for hydrated cement pastes of various ages. It was confirmed that sulfur is universally distributed throughout calcium silicate hydrate gel regions. Local calcium to silica ratios of the gel ranged generally between 2 and 3, considerably higher than had been expected. A number of morphological features found in hydrated cement pastes were interpreted in the light of the chemical compositions determined.

Introduction

This paper is the result of an investigation into the feasibility of employing a scanning electron microscope-energy dispersive x-ray spectrometer combination to determine the approximate composition of particles and areas of interest in hydrated cements as revealed by the scanning electron microscope (SEM). Recent SEM studies of hydrated cement pastes and related materials suggest that the microstructure of these important substances is far more complex than had been previously appreciated. Proper interpretation and understanding of the microstructural features requires that the approximate composition or at least the chemical nature of the particles and other microstructural units be known.

Commercially available energy-dispersive spectrometers are now made to fit most SEM models. They are particularly adapted to the present purpose because they do not require flat specimen surfaces, and function well on the rough fracture surfaces usually examined in studies of hydrated cements. Rapid progress is being made in the capabilities of these units, and more refined and much more convenient analyses than reported here should be possible in the near future.

Instrumentation

Recent discussions of the theory and mode of operation of energy-dispersive x-ray spectrometrers have been given by Russ (1), Frankel and Aitken (2) and Sutfin and Ogilvie (3), among others, and the proceedings of a recent symposium on the subject are now available (4). A diagram of such a spectrometer is given as Figure 1.

Briefly, the device functions to detect, count, and allocate to energy classes the x-rays produced from a small, local region of the specimen selected for analysis. When used in conjunction with the SEM the detector takes the form of a cryogenic semiconductor

mounted in the SEM sample chamber near the specimen. The electron beam is focused on the area of interest; x-rays are generated by the sample and interact with the detector to generate electrical pulses that are proportional in height to the energies of the photons detected. A multichannel analyzer is used to sort the pulses into narrow individual energy ranges ("channels"), and to accumulate the count of pulses assigned to each channel. Equipment is provided to record and display the resulting distribution of counts vs. x-ray photon energy. The elements present in the area examined are readily identified by reference to their characteristic x-ray spectra. The Kα lines are readily observed for most of the elements of interest in hydrated cements, except for a few heavy elements for which L lines may be used. Commercial systems using thin windows can readily detect elements as low as Na (atomic number 11). The spectra are displayed continuously on a cathode ray tube while being accumulated, and after completion of the counting the data may be read out numerically on a teletypewriter, plotted graphically on an x-y recorder, or transmitted directly or indirectly to a computer for further processing.

A number of modes of operation of the SEM - spectrometer combination are possible. The simplest method is to excite the spectra by operating the electron beam in a fixed location at any point on the specimen selected for analysis. Alternatively, one can cause the electron beam to travel in a raster pattern over a designated area on the surface of the specimen and thus record x-rays generated from the entire selected area. It is also possible to record the intensity of x-rays of a single element along a repeatedly scanned line, or to obtain a display of the pattern of distribution of an element over the prescribed area. In the present work essentially all of the data were secured from stationary excitation at a fixed point, so that the analysis refers to the composition of a small zone surrounding the impacted point.

Unfortunately, while the diameter of the electron beam can be regulated by the operator and is usually maintained at several hundred Å, the beam penetrates the sample and spreads laterally, exciting

x-rays from a considerable volume of solid material. A number of workers have dealt with the problem of calculating the beam spread within a non-porous solid of homogenous composition, primarily with respect to electron probe applications (5,6,7). The extent of spreading is a function of the voltage used to generate the electron beam, of the beam current, and of the density and chemical composition of the specimen. Russ and Kibaya (8) measured the effective spread of the electron beam in an SEM, using stainless steel specimens. For the FeKα peak, they found x-rays generated from an effective diameter ranging from 0.3 μm for 15 keV excitation and low beam current, to as much as 5 μm for 50 keV excitation and very high beam currents. In the present work, it is estimated from calculations based on two of the above treatments (5, 8) that the effective diameter for x-ray generation for the elements of interest (Ca Kα and less energetic radiation) is of the order of 1.5 μm, i.e. that the radius of effective influence of a stationary electron beam is about 0.75 μm from the impacted point. These calculations assume that the local region is essentially solid; the presence of void space would extend the dimensions of the effective zone.

Experimental Details

All of the analyses in the present work were carried out using a Cambridge Instrument Company Stereoscan IIa scanning electron microscope fitted with a Kevex Corporation lithium-drifted silicon detector unit coupled to a multichannel analyzer and display unit manufactured by the Northern Scientific Corporation. The energy resolution of the x-ray unit was approximately 215 eV. Specimens were initially prepared for SEM observation using a two step electrical conductivity coating consisting of carbon and a gold-palladium alloy. Subsequently it was determined that a spectral line of gold interfered with the analysis for sulfur, and chromium was substituted for the gold-palladium without significant loss of apparent resolution capability in SEM observation.

The specimens used were of two kinds. Standards of compounds of known stoichiometry were available as powders, and were prepared for observation and analysis by mounting the powders on double-coated cellophane tape previously affixed to the SEM specimen stubs. Specimens of hardened cement paste were fractured after drying to yield blocks of the order of 1 cm on a side, which were mounted to the stubs with Duco cement and then coated. Silver conducting paint was applied judiciously to assure conduction to ground.

In general, the observations consisted of a) SEM observation of the specimen, and selection of local regions for analysis, b) photographing the region, c) placing the beam spot on the preselected site and adjusting the electron beam for efficient x-ray production, and d) counting. All of the observations were carried out at 20 keV.

To secure proper x-ray analyses it is important to assure a direct straight-line path is available between the spot chosen for analysis and the x-ray detector. Any overhanging or blocking regions of the rough fracture surface that the x-rays would have to pass through would alter the relative quantities of the photons of different energies by differential absorption and fluorescence effects. With proper operator care, it is usually possible to avoid such problems by tilting or rotating the specimen stage.

Calibration and Analysis Scheme

Since the objective of this study was to determine the approximate chemical composition of local regions on a rough, porous, complex fracture surface, it was decided to set up the analysis in terms of ratios rather than to attempt to determine absolute compositions. In conformity with the usual conventions in cement chemistry, the ratios are expressed as oxide ratios rather than as element ratios.

A suite of pure, well-characterized samples of synthetic cement minerals and cement hydration compounds was assembled by the author through the courtesy of L. E. Copeland and his associates of the

Portland Cement Association and of Horace Berman, formerly of the National Bureau of Standards. These were supplemented by several additional samples prepared in the author's laboratory and by a few pure minerals. These propective standards were checked by x-rav diffraction, examined critically by SEM observation to insure that they appeared microscopically homogeneous, and then tested by repeated x-ray spectra taken on different grains. All but a few proved quite homogeneous on a local scale and were judged suitable for use.

X-ray spectra were obtained for each of these standards in the form of quantitative count readings in each of two hundred channels covering the energy range from zero to 10 keV in steps of 50 eV per channel. Each spectrum was normally accumulated for a period of 100 seconds of counting, the electron beam being positioned on a single spot. The beam current used was sufficient to accumulate on the order of ten to thirty thousand counts in the channel marking the center of the Ca Ka peak. For each spectrum, the counts of the channels marking the centers of the Ka peaks of calcium, silicon, sulfur, and aluminum were noted. No background corrections were made. Ratios of these gross peak heights were computed for calcium compared with each of the other elements. Averages of these gross peak height count ratios were compiled from replicate spectra taken from 4 to 5 separate grains of each compound. The resulting average count ratios were plotted against the known oxide composition ratios of the standards to yield the calibration curves of Figures 2, 3, and 4, respectively.

A number of observations are evident with respect to these figures. In all cases the count ratios are linearly related to the composition ratios, at least in the range of compositions examined. The slopes of all of the straight lines are reasonably close to unity. The intercepts are small for the CaO/SiO_2 and CaO/SO_3 comparisons, but fairly large for the CaO/Al_2O_3 calibration line. Compounds having the same composition ratios for particular pairs of elements but different residual compositions show essentially identical

count ratios for the common elements. For example, tetracalcium aluminate-13-hydrate (C_4AH_{13}), tetracalcium aluminate monocarbonate-11-hydrate ($C_3A{\cdot}CaCO_3{\cdot}11H_2O$), and tetracalcium aluminate monosulfate-12-hydrate ($C_3A{\cdot}CaSO_4{\cdot}12H_2O$) all have CaO/Al_2O_3 ratios of 4.0 and all have approximately the same count ratio, as indicated in Figure 4. This observation suggests that interelement effects are not likely to be troublesome in the cement systems.

The utility of these calibration curves for determining the local composition of particles in cement pastes and other complex systems is apparent, provided that the deviations of individual trials from the mean count ratios is not too great. That this is the case is indicated by the data for repeat counts tabulated in Table I, which conveys the range of individual variation normally encountered, and the repeatability of the counting process at different times. While no formal statistical analysis of this and much additional complementary data was attempted, it seems clear that the precision of the determinations is quite satisfactory for the purpose proposed. In this connection, due caution always needs to be paid to the provision of a clear path from the site selected for observation to the x-ray detector, as previously mentioned. Also, it was observed that occasionally electrical malfunction or instrumental error produces a widely deviant count ratio; however, repeat trials on a single spot or movement to another spot in the same particle usually discloses the deviation and the offending count ratio may be ignored. Since under appropriate conditions a single count can be completed in a few minutes replicate analyses do not constitute a burden.

Analyses of Hydrated Cement Pastes

In the following section, a number of micrographs illustrating various characteristic features of hydrated cement pastes are discussed in terms of the analysis secured from particular spots, as indicated by the markers. Each cited analysis represents an average of three to five replicate determinations on the same spot. The actual compositional

ratios cited were calculated from the count ratios by linear equations fitted the calibrations previously given. Analyses representing significant extrapolation from the range of the calibration curves are reported as approximations to the nearest one-half ratio unit. The validity of these approximations is unknown, but the relative values should be correct.

Figure 5 shows a characteristic microstructure found in most hydrated cement paste, a spherulitic cluster of calcium silicate hydrate, found in an 0.6 W:C ratio paste hydrated for 185 days at 40°. Morphological units of this type have been previously reported in cement paste (9) and in pastes of dicalcium silicate (10), and their growth was explained by Williamson (11) on the basis of constitutional supersaturation. The analysis indicates a CaO/SiO_2 mole ratio of 2.08, substantially that of dicalcium silicate. There is a definite spectral response for sulfur, and the apparent CaO/SO_3 ratio is about 13.5, judged from a linear extrapolation of the calibration curve of Figure 3. While no direct calibration is available for the SiO_2/SO_3 mole ratio, the two ratios above lead algebraically to an estimate of 6.5 for this ratio. Copeland et al (12) determined that sulfur added to C_3S in the form of gypsum was incorporated in the resulting calcium silicate hydrate gel in amounts corresponding to a maximum SiO_2/SO_3 mole ratio of 6.3. The nearly precise agreement of the present data is probably fortuitous. Nevertheless, as will be apparent subsequently, sulfate contents of this order of magnitude are universal in the calcium silicate hydrate gel areas analyzed. This is in accord with the previous indications by Kalousek (13) and by Copeland et al that this element is normally incorporated in solid solution within the gel structure.

Figure 6 shows a field consisting mostly of clusters of relatively short fibrous particles, the clusters being of the order of 2 μm in diameter. Such clusters seem particularly characteristic of observations made in the earlier stages of hydration. The paste represented here is an 0.6 water:cement ratio paste hydrated for 7

days at 6°C. Such fibers are sometimes seen to grow from the surface of cement or C_3S grains, but in the present case it appears that they represent the growth of precipitation nuclei from solution. The analyses of the two points indicated on the micrograph yield CaO/SiO_2 ratios of the order of 2.3, and CaO/SO_3 ratios similar to that of the longer-fibered spherulites of Figure 5. The very thin flat filmy plate observable in the upper right-hand corner is apparently calcium hydroxide, although a specific analysis of this feature was not made.

The presence of calcium hydroxide within the hardened cement paste is noticeable even at early ages. Figure 7 shows an 0.6 water:cement ratio paste hydrated at 24°C for 1 day. The roughly half-micrometer thick plate in the center of the figure, marked by the erect triangle, is clearly calcium hydroxide. Somewhat surprisingly the rather large needle-shaped particles just above and to the right of this plate (indicated by the inverted triangle) also seem to be calcium hydroxide. Examination of another area marked by such needle-shaped particles in the extreme left-hand portion of the figure, made by rastering a very small square pattern covering the area of contact between the two crossed needles, gave a substantially identical analysis. It is apparent from the lack of sulfur that these particles are definitely not ettringite, and the lack of silica suggests that they are not a variety of calcium silicate hydrate.

The analysis of the calcium silicate hydrate gel region near the bottom of Figure 7 shows a CaO/SO_3 ratio substantially identical to that previously indicated as characteristic for gel, but a somewhat higher CaO/SiO_2 ratio of 2.9. It appears that the CaO/SiO_2 ratio to be found in the gel varies usually between 2 and 3. Figure 8 shows a typical example of a field from another young paste (0.6 water:cement ratio, hydrated 4 days at 6°C) in which local analyses indicate CaO/SiO_2 ratios of 2.9 and 2.3, respectively in adjacent regions.

As cement paste matures calcium hydroxide becomes an increasingly prominent constitutent. Large crystalline masses grow through regions of the paste, incorporating previously existing particles of gel and of unhydrated cement. The crystals often give no apparent indication of the presence of inclusions from the smooth appearance of their surfaces, and it is true that in some areas such inclusions are minor in amount. One good indication of the presence of such hidden inclusions seems to be the detection of sulfur radiation from the suspected area. It seems clear from the previously cited analysis, and has been abundantly confirmed by many additional analyses, that sulfur is always present in calcium silicate hydrate gel generated from sulfate-interground portland cement. The analyses of Figure 7 and other similar results suggest that sulfur is usually excluded from the pure crystals of calcium hydroxide formed at early stages of hydration. Thus the detection of sulfur in a massive calcium hydroxide zone implies that gel formed initially and was later encapsulated by the growing lime crystal. Of course, the presence of significant amounts of silica within the seemingly pure lime crystal also serves to signal the presence of gel, and the combination of the two in roughly the appropriate proportions for gel seems to provide a clear indication of its presence.

Figure 9 shows an indication of a more or less typical local region of calcium hydroxide growth in mature paste. The specimen is an 0.6 water:cement ratio paste hydrated for 185 days at 40°C. The large blocky crystal in the upper half of the figure (presumably broken in two during the fracture incident to preparation of the specimen), shows visible gel inclusion. It does, however, show detectable sulfur and an appreciable silica content. The flat appearing surface of the lime crystal in the lower left-hand portion of the figure (indicated by the triangular mark) is close to apprarent layers of gel; thus the sulfur and silica contents are not particularly helpful in interpretation. The analysis for the gel itself, centered at the square mark, shows a composition within the

range for gel previously observed, although the sulfur content appears slightly lower than the average.

Figure 10 conveys a more or less similar picture. This is a field from an 0.4 water:cement ratio paste hydrated for one year at 6°C. The analysis for the lime crystal (triangular mark) is similar to those of Figure 9, as is the analysis for the gel region (round mark), except that the sulfur content of the gel in this case is a little higher than usual.

An idea of the extensive intermingling of calcium hydroxide and cement gel in many areas of mature paste is provided in the next two figures. Figure 11, taken from a paste of water:cement ratio 0.4 hydrated for 1 year at 6°C, yielded analyses indicating that the upper, massive appearing broken crystal is largely pure calcium hydroxide: that the smooth, flat area in the foreground is calcium hydroxide with some underlying or incorporated gel; and that the porous areas indicated by the triangular mark are essentially calcium silicate hydrate gel with a little admixed lime. Figure 12 was taken from an 0.6 water: cement ratio paste hydrated for 318 days at room temperature. This particular specimen was coated with gold-palladium, so that sulfur analysis is not available, but the calcium:silica ratios are of interest. An analysis made on an area of gel just above the figure gave a CaO/SiO_2 ratio of 2.9, within the normal range of gel previously indicated. The two analyses indicated for gel areas near the bottom of the figure yielded ratios somewhat higher than the normal range, close to 4; suggesting that some extra lime is contributing to the count. Four closely spaced analyses indicated on the fractured stratum emerging from the mass at the right-hand side of the picture all yield CaO/SiO_2 ratios between 7 and 11. This confirms the visual indication that despite the smooth surfaces present (where the plates are not fractured), many areas that appear to be pure crystals of calcium hydroxide do in fact incorporate significant amounts of gel.

It is generally appreciated that hydration of portland cement is often less than complete, even after prolonged periods. Thus residual unhydrated portions of cement grains ought to be visible occasionally in fracture surfaces of pastes. Comparatively few such grains were identified in the present study.

When an individual remnant grain was found, it was not always evident whether the grain represents the original unchanged cement mineral or a pseudomorphic "inner" hydration product. Figure 13 shows such a grain. The analysis indicates that no sulfur is detected, and the CaO/SiO_2 ratio observed is sufficiently close to 3 to suggest that it is a remnant grain of C_3S. The paste is young enough (0.6 water:cement ratio, hydrated at $6^{\circ}C$ for 4 days) that this is not unreasonable. On the other hand there appears to be at least a surface layer of very fine, mostly needle-shaped particles, which appear to indicate at least partial hydration. Figure 14 is a grain found in a much more mature paste (0.6 water: cement ratio, hydrated for 185 days at $40^{\circ}C$) which appears to be β-C_2S from the analysis. However, both areas analyzed yield indications of more than a trace of sulfur, a feature not easily explained.

The relationship that may be developed at the perimeter of a hydrating cement grain and the nature of reaction products produced there has been a subject of considerable interest. Williamson (10) has discussed the formation of 'inner' hydration product within the perimeter of the original grain which is said to constitute a zone of pseudomorphous hydration: this is said to be surrounded by a so-called "columnar" zone of outer product growing outward from the former rim of each grain. Indications for the existence of such zones seem to be quite rare in the many fields examined in the present research, perhaps because of overgrowth by other materials. However, one field which appears to perhaps reflect such a situation is given in Fig. 15, for a quite immature paste (0.6 water:cement ratio, hydrated for 2 days at $6^{\circ}C$). Fracturing of this weak paste

has apparently disturbed the local spatial relationships considerably, but the left-hand portion of the figure shows a wedge-shaped unit which might be taken as a piece of inner product with a portion of its rim of reaction product clinging above it. Figure 16, which shows fine detail of this area confirms the porous nature of the supposed inner product, showing pores of the order of perhaps 500 Å separating poorly defined grains. The analysis for this area show no sulfur present at all, and CaO/SiO_2 ratios are close to 3, suggesting that the original grain was tricalcium silicate. Approximately half a micrometer above the "rim", analyses of the center of what might be taken as the columnar zone show that here some sulfur is present and that an enrichment in calcium has occurred. Analyses taken above the point where the columnar zone fades into the general calcium silicate hydrate gel groundmass show the typical composition for ordinary sulfate-substituted calcium silicate hydrate gel. It should be noted that the apparent "columnar zone" is only a micrometer or so thick, much thinner than the thick columnar layers postulated by Williamson.

Discussion

Several generalizations drawn from the analytical information presented in this paper are worthy of further discussion.

First, it was noted previously that local analyses for areas of paste identified as calcium silicate hydrate gel show CaO/SiO_2 ratios between 2 and 3, except for a few areas, apparently influenced by nearly calcium hydroxide, that show even higher values. This is in contrast with estimates of CaO/SiO_2 ratios previously reported in the literature as reflecting the composition of gel in pastes of hydrated C_3S or C_2S. In such studies the amounts of unhydrated compound and of calcium hydroxide are determined and the composition of the calcium silicate hydrate gel calculated by difference of these elements from the known overall composition of the paste. Typical

results are given by Kantro, Weise, and Brunauer (13), who find a range between 1.35 and 2.1 for C_3S pastes varying in age from 1 day to more than 1 year, and a range of 1.0 to 1.8 for C_2S pastes ranging in age from 1 day to almost 5 years. Locher (14) reported essentially similar compositions for C_3S pastes, with his reported range being slightly higher (1.6 to 2.3) if the calcium hydroxide determination by TGA is used in the calculations. The apparent contradiction between these indirect calculations and the present local analyses on hydrated portland cement pastes certainly invites further investigation.

Secondly, it is worth while reemphasizing that the areas identified as calcium silicate hydrate gel always yielded measureable spectral peaks for sulfur. The few areas, such as those shown in Figure 16, that appeared to be "inner" product, i.e. material hydrated, if at all, only by topotactic reaction did not show the presence of sulfur. Only reaction product generated by a through-solution mechanism is likely to incorporate an impurity such as the sulfate ion so uniformly over all regions of the gel formed.

Finally, in contrast to the useful information derived with respect to the distribution of sulfur in the hydrated pastes, that obtained in this study with respect to aluminum distribution was quite disappointing. The Al Kα peak is difficult to resolve completely from that of silicon when aluminum is present only in small amounts. In separate x-ray diffraction studies of most of the pastes examined it was confirmed that both ettringite and tetracalcium aluminate monosulfate-12-hydrate were present in small amounts within the pastes examined. However, in the SEM investigation areas in which the presence of these compounds was suspected were observed only very infrequently on the fracture surfaces obtained, and in general these areas could not be analyzed quantitatively. It

seems that a more elaborate analytical procedure and a spectrometer of somewhat better resolution will be required to yield meaningful information on the distribution of aluminum in hydrated cement pastes.

Conclusions

1. Rapid identification and approximate quantitative analysis of microstructural features observed in hydrated cements by SEM may be easily accomplished by energy-dispersive x-ray spectrometer attachment to the instrument.
2. Ratios of gross peak heights observed for Ka peaks are linear functions of the corresponding ratios of elements for calcium as compared to silicon, sulfur, and aluminum. Interelement effects seem not to be important.
3. Observed CaO/SiO_2 ratios for local areas identified as calcium silicate hydrate gel range broadly between 2 and 3, and are thus higher than those normally considered to be characteristic of this substance.
4. Sulfur is identified as a minor constituent in all regions identified as calcium silicate hydrate gel (in hydrated portland cement), but is not present within small, well-formed calcium hydroxide crystals. Its detection in large masses of calcium hydroxide is an indication that the calcium hydroxide has grown through an area in which calcium silicate hydrate gel was previously deposited.

Acknowledgements

This research was supported by the Indiana State Highway Commission and the Federal Highway Administration through the Joint Highway Research Project, Purdue University. The analytical work was carried out using the SEM and associated x-ray spectrometer facilities of the Analytical Instrumentation Laboratory, Engineering Experiment Station, Georgia Institute of Technology. The author expresses his gratitude to John Brown, Head of the Laboratory, and to James L. Hubbard and Larry Glassman for their exceedingly fruitful collaboration. Thanks are due to L. E. Copeland and to Horace Berman for gifts of pure cement and hydrated cement compounds which served as analytical standards.

REFERENCES

1. J. C. Russ, Scanning Electron Microscopy/1971 (Proc. 4th Annual S.E.M. Symposium, Chicago) 65 (1971).

2. R. S. Frankel and D. W. Aitken, Applied Spectroscopy 24 557 (1970).

3. L. V. Sutfin and R. E. Ogilvie, Scanning Electron Microscopy/1970 (Proc. 3rd Annual S.E.M. Symposium, Chicago) 17 (1970).

4. J. C. Russ, coordinator, Energy Dispersion X-Ray Analysis, S.T.P. 485, Amer. Soc. Testing and Matls., 285 pp (1971).

5. S. J. B. Reed, X-Ray Optics and Microanalysis (Proc. 4th Intl. Congress, Orsay, 1965) 339 (1966).

6. V. E. Cosslett, X-Ray Optics and Microanalysis (Proc.4th Intl. Congress, Orsay, 1965) 85 (1966).

7. H. E. Bishop, X-Ray Optics and Microanalysis (Proc. 4th Intl. Congress, Orsay, 1965) 112 (1966).

8. J. C. Russ and A. Kibaya, Scanning Electron Microscopy/ 1969 (Proc. 2nd Annual S.E.M. Symposium, Chicago, 1969) 57 (1969).

9. S. Diamond, Scanning Electron Microscopy/1970 (Proc. 3rd Annual S.E.M. Symposium, Chicago, 1970) 385 (1970).

10. R. B. Williamson, Solidification of Portland Cement, Report No. UC-SESM 70-23, University of California, Berkeley 109 pp (1970).

11. R. B. Williamson, J. Crystal Growth 3,4 787 (1968).

12. L. E. Copeland, E. Bodor, T. N. Chang, C. H. Weise, J. P.C.A. Res. and Dev. Labs. 9 61 (1967).

13. D. L. Kantro, C. H. Weise, and S. Brunauer, Symposium on Structure of Portland Cement Paste and Concrete, Highway Res. Bd. Special Report 90, 309 (1966).

14. F. W. Locher, Symposium on Structure of Portland Cement Paste and Concrete, Highway Res. Bd. Special Report 90, 300 (1966).

15. G. L. Kalousek, Materials Research and Standards 5 292 (1965).

TABLE 1

Illustration of the Typical Variation of Individual Count Ratios
Ca Kα/ S Kα Ratios in Ettringite

Ettringite I (NBS)		Ettringite II (PCS)
July 1, 1970	July 28, 1970	July 30, 1970
2.01	1.95	1.98
1.93	1.98	1.91
1.95	1.95	1.98
1.91	1.99	----
----	1.92	----
Aver. 1.95	Aver. 1.96	Aver. 1.96

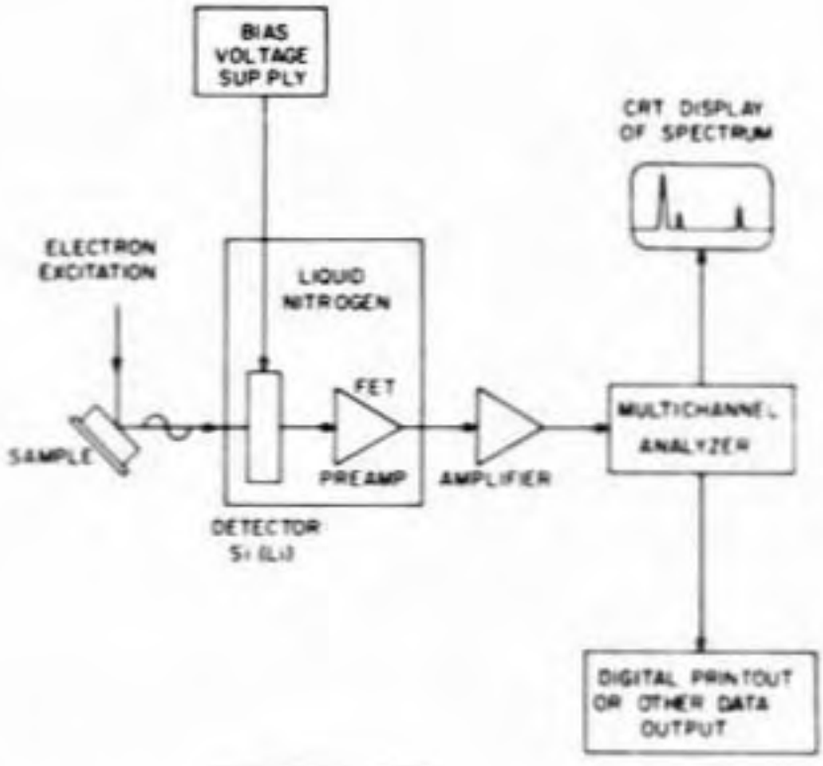

FIG. 1 Schematic diagram of energy-dispersive x-ray spectrometer.

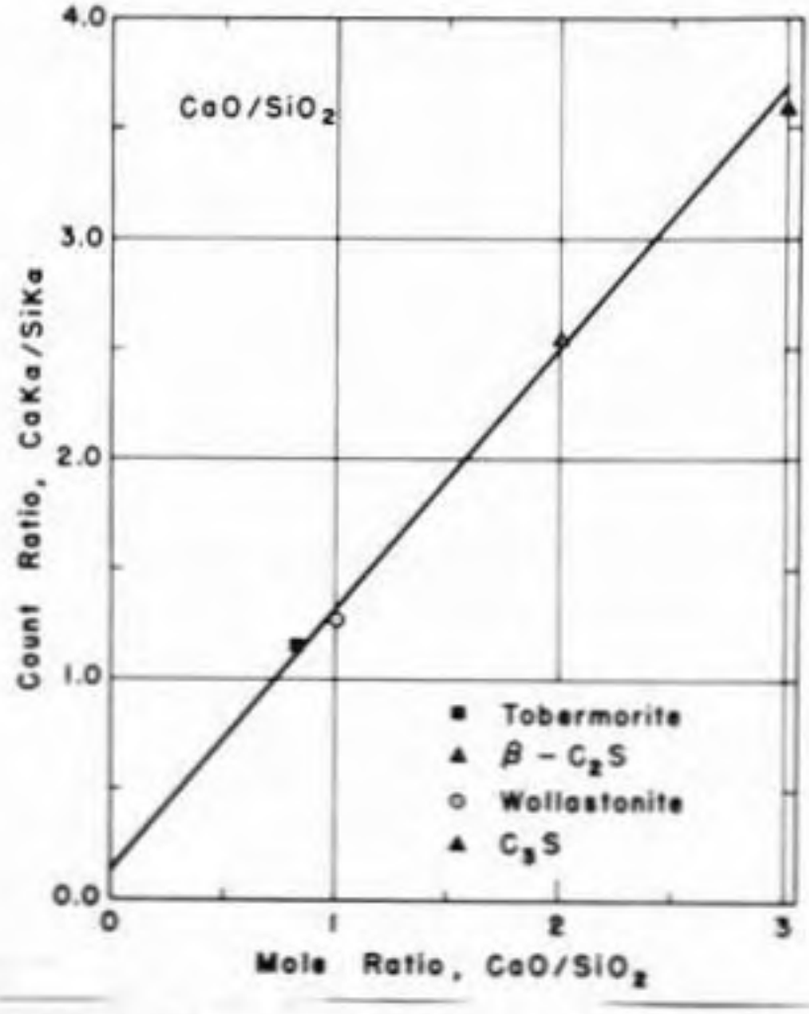

FIG. 2 Calibration for determination of CaO/SiO_2 ratio.

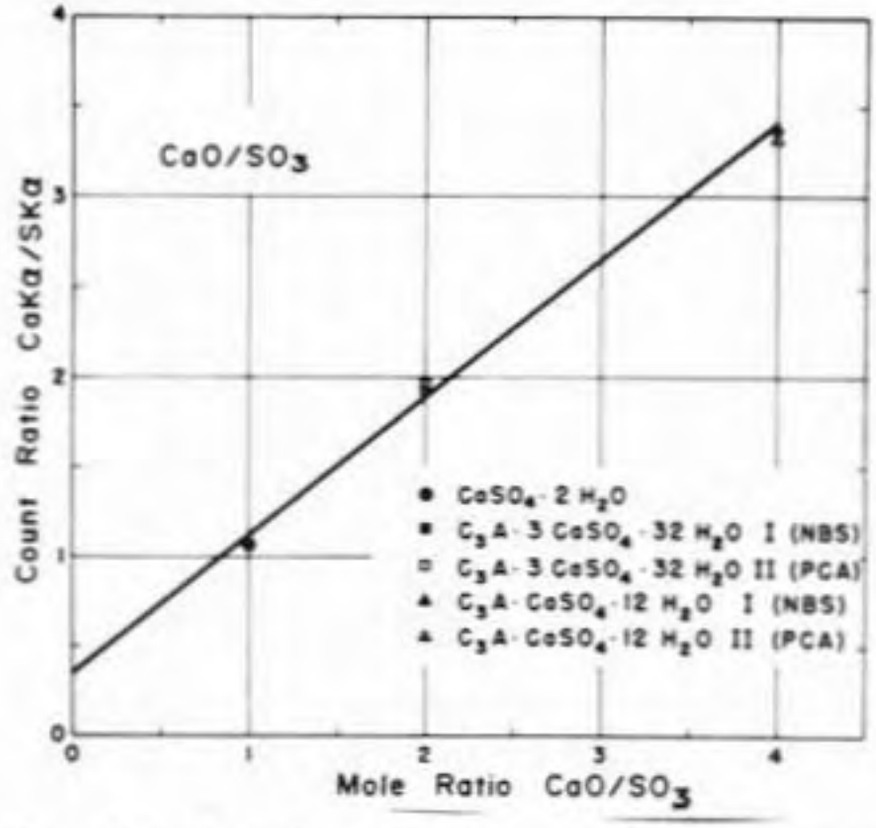

FIG. 3 Calibration for determination of CaO/SO_3 ratio.

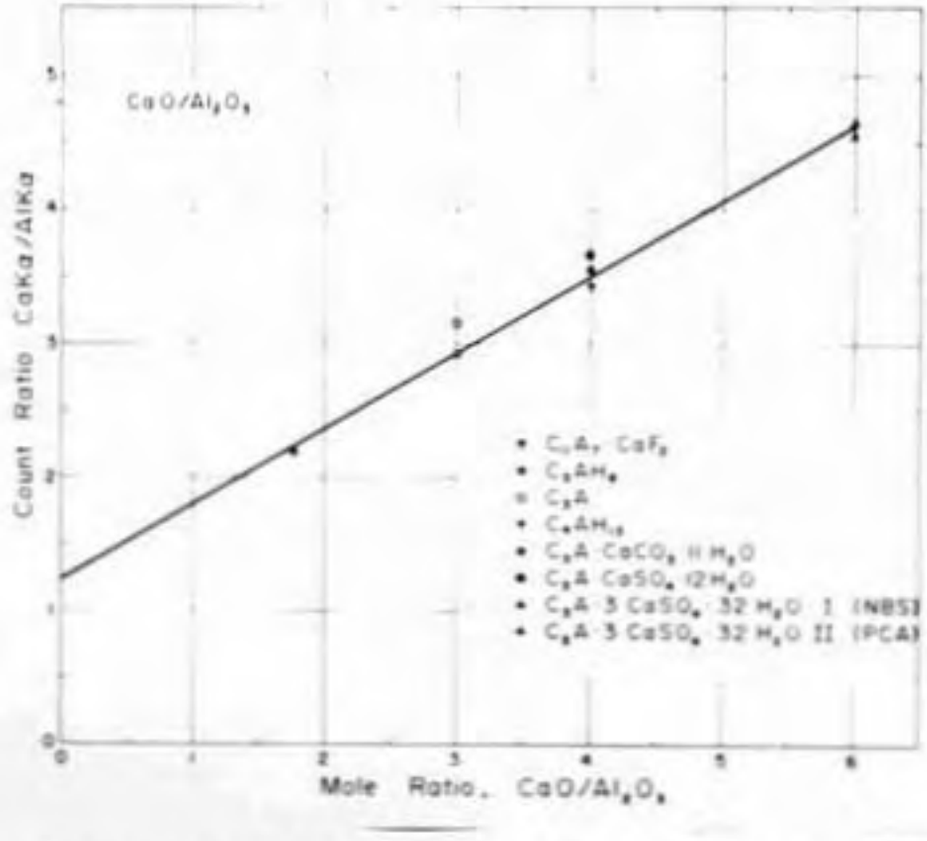

FIG. 4 Calibration for determination of CaO/Al_2O_3 ratio.

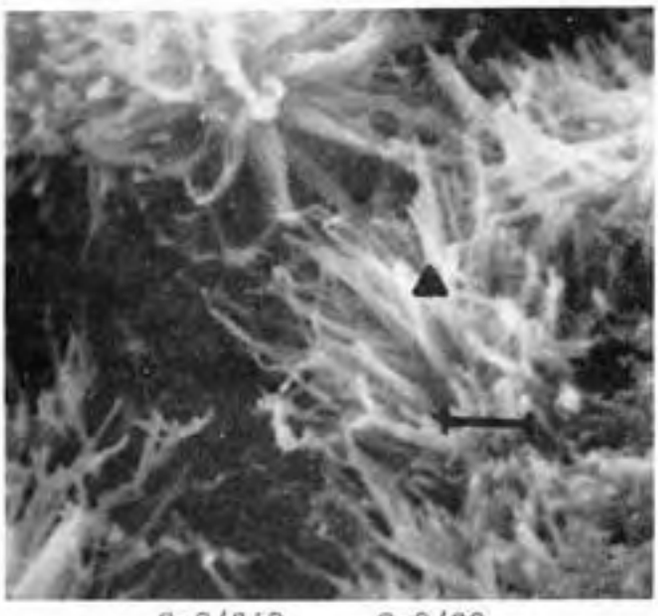

	CaO/SiO_2	CaO/SO_3
▲	2.08	13.5

FIG. 5

Spherulitic cluster of calcium silicate hydrate gel. W:C 0.6, hydrated 185 days at 40°C.

	CaO/SiO_2	CaO/SO_3
●	2.42	13.5
▲	2.27	12.5

FIG. 6

Short-fibered clusters of calcium silicate hydrate gel. W:C 0.6, hydrated for 7 days at 6°C.

	CaO/SiO_2	CaO/SO_3
▲	30.	no SO_3
●	35.	no SO_3
▼	36.	no SO_3
■	2.91	13.5

FIG. 7

Calcium hydroxide plates formed at early stage of hydration. W:C 0.6 hydrated 1 day at 24°C.

	CaO/SiO_2	CaO/SO_3
●	2.88	12.
▲	2.30	10.5

FIG. 8

Calcium silicate hydrate gel. W:C 0.6, hydrated 4 days at 6°C.

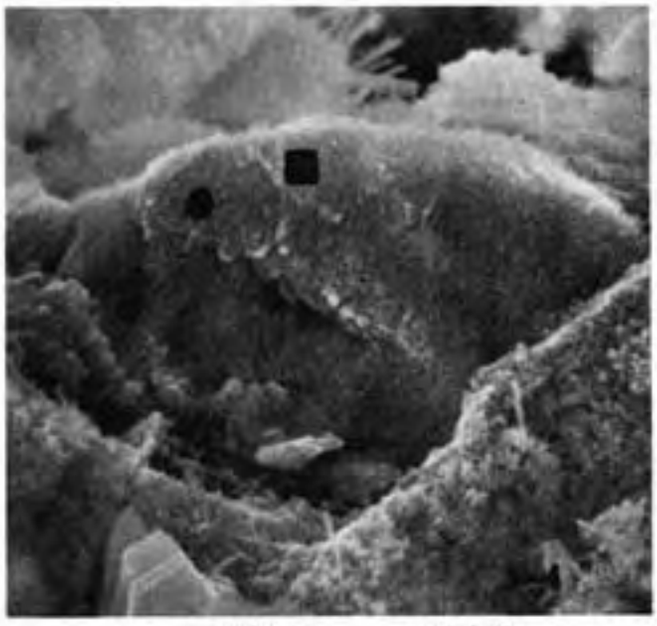

	CaO/SiO_2	CaO/SO_3
●	3.15	no SO_3
■	3.17	no SO_3

FIG. 13

Remnant grain of C_3S. W:C 0.6, hydrated for 4 days at 6°C.

	CaO/SiO_2	CaO/SO_3
●	2.06	14.
▲	1.92	15.

FIG. 14

Apparent remnant grain of β-C_2S. W:C 0.6, hydrated 185 days at 40°C.

FIG. 15 (Above)
Region surrounding possible fragment of "inner product" with apparent columnar zone above. W:C 0.6, hydrated 2 days at 6°C.

FIG. 16 (Right)
Higher-magnification view of area outlined above.

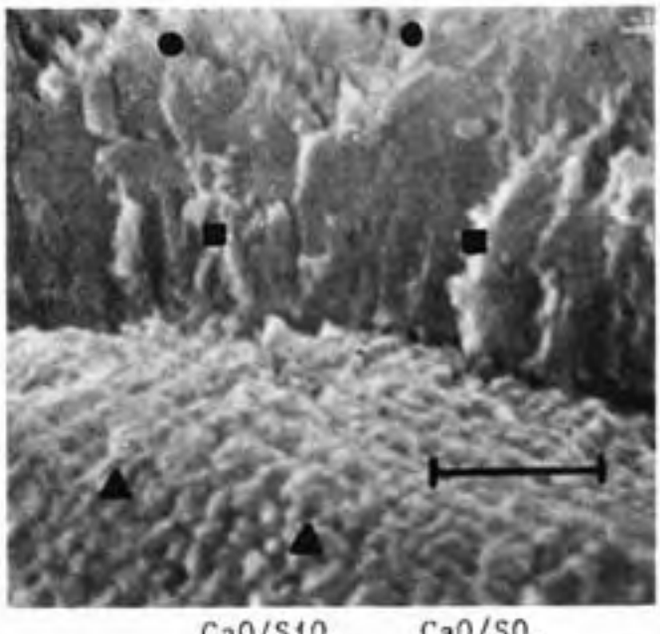

	CaO/SiO_2	CaO/SO_3
▲	3.02	no SO_3
▲	2.90	no SO_3
■	3.54	19.5
■	3.43	16.
●	2.48	12.
●	2.40	11.5

	CaO/SiO_2	CaO/SO_3
●	16.5	27.
▲	10.	24.
■	2.85	16.5

FIG. 9

Massive calcium hydroxide crystal. W:C 0.6, hydrated 185 days at 40°C.

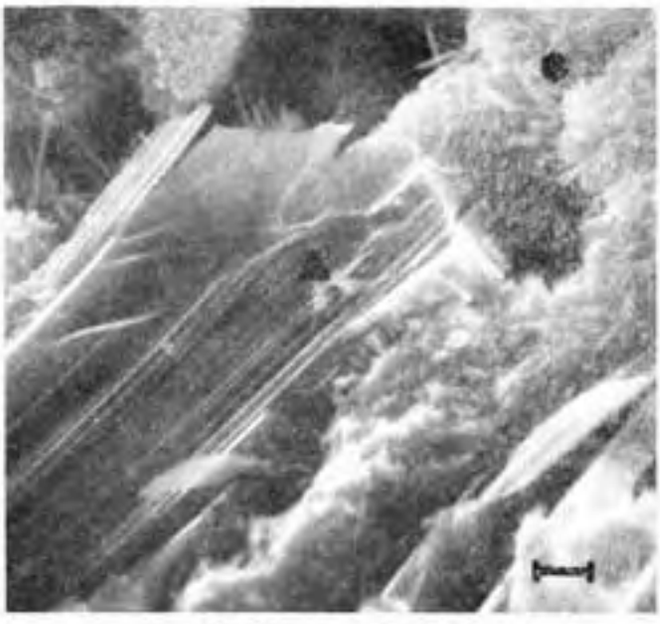

	CaO/SiO_2	CaO/SO_3
▲	13.5	26.
●	2.72	9.5

FIG. 10

Calcium hydroxide crystal growing through calcium silicate hydrate gel W:C 0.4, hydrated for 1 year at 6°C.

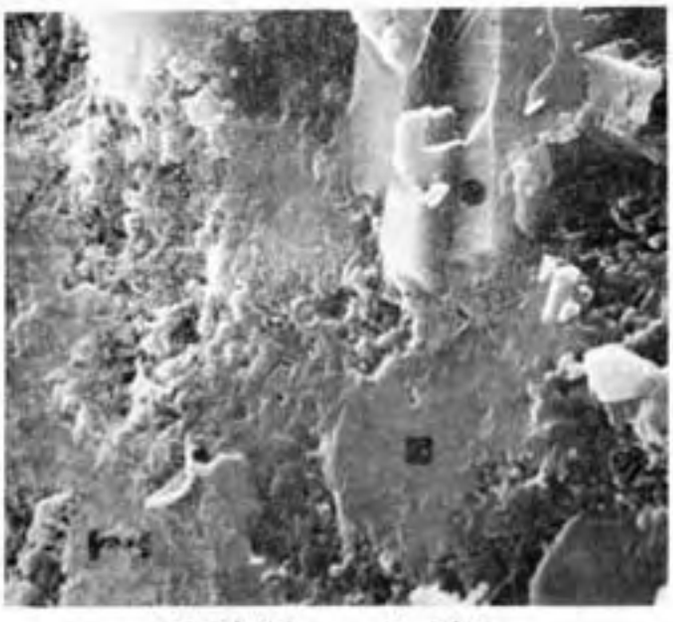

	CaO/SiO_2	CaO/SO_3
●	14.	no SO_3
■	9.5	no SO_3
▲	3.26	19.

FIG. 11

Intermingling of calcium hydroxide and calcium silicate hydrate gel. W:C 0.4, hydrated for 1 year at 6°C.

	CaO/SiO_2	
■	8.	● 7.
▲	8.	● 3.6
▼	11.	○ 4.2

FIG. 12

Growth of calcium hydroxide crystals through calcium silicate hydrate gel. W:C 0.6, hydrated 318 days at 24°C.

LIST OF FIGURES